

Blazars as neutrino factories

Chiara Righi

Università degli Studi dell'Insubria
INAF - OA Brera

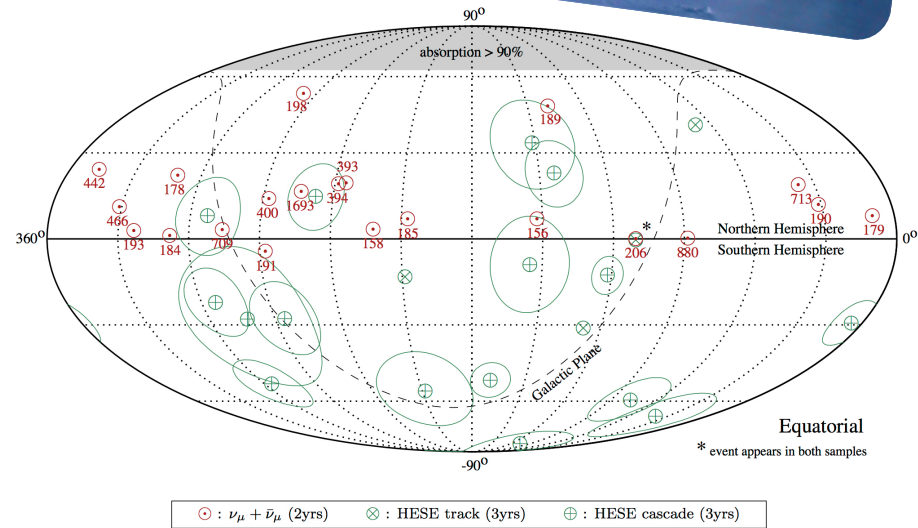
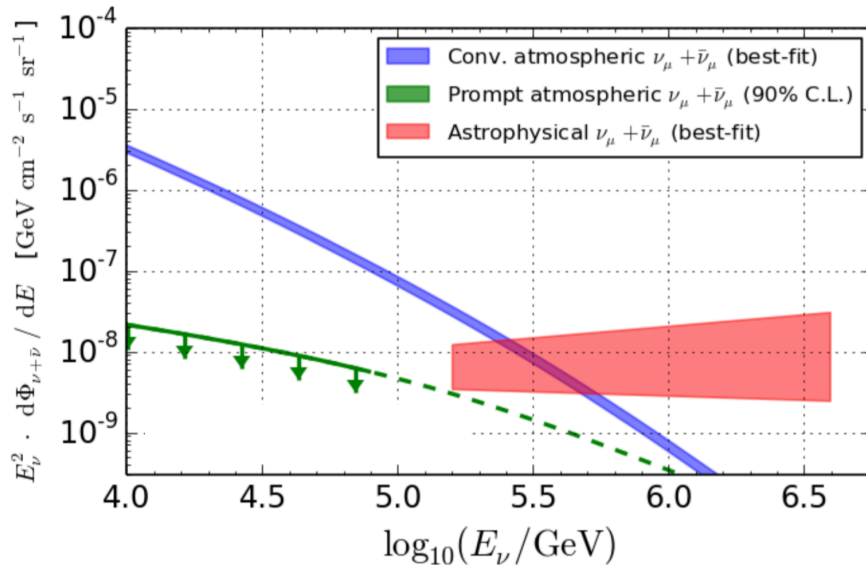


Collaborators: F. Tavecchio, G. Ghisellini, M. Landoni, L. Pacciani, S. Inoue, ...

Discovery of high-energy neutrinos by IceCube

~60 events since 2010
above 60 TeV

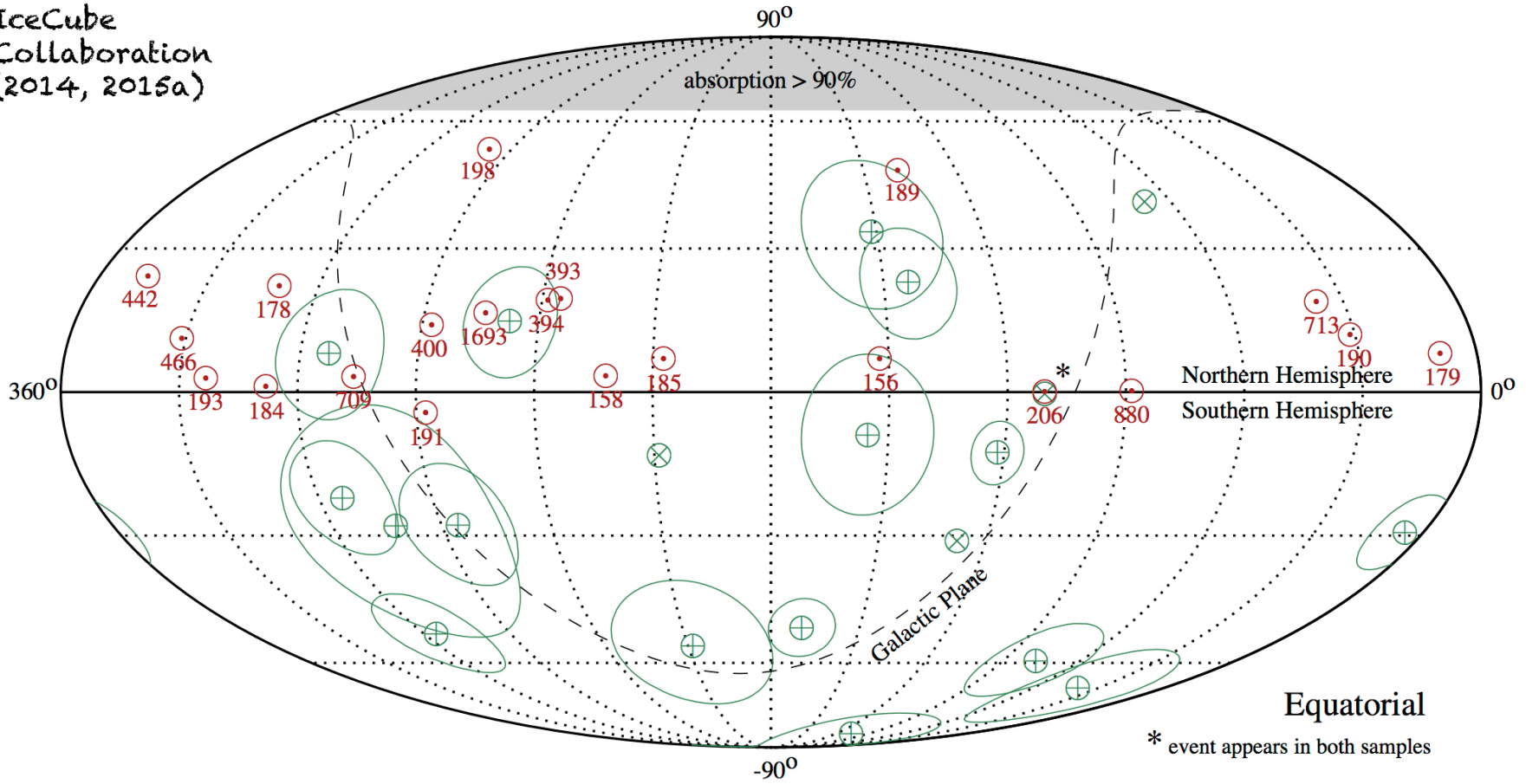
Aartsen et al. 2016



Who is producing these neutrinos?

Searching for sources

IceCube
Collaboration
(2014, 2015a)



⊙ : $\nu_\mu + \bar{\nu}_\mu$ (2yrs)
 ⊗ : HESE track (3yrs)
 ⊕ : HESE cascade (3yrs)

* event appears in both samples

High-energy neutrino production

Relativistic protons!!

$$p + p \rightarrow \pi + X$$

$$p + \gamma \rightarrow \pi + X$$

$$\pi^{\pm} \rightarrow \mu^{\pm} + \nu_{\mu} \rightarrow e^{\pm} + \nu_e + 2 \nu_{\mu}$$

$$\pi^0 \rightarrow \gamma + \gamma$$

$$E_{\nu} \sim E_p / 20$$

1:1:1
after propagation

High-energy neutrino production

Relativistic protons!!



Our galaxy
Star-forming Galaxy
AGN winds
Low-energy radiogalaxies (FRO)

High-energy neutrino production

Relativistic protons!!



Our galaxy
Star-forming Galaxy
AGN winds
Low-energy radiogalaxies (FRO)



Protons accelerated inside the SNR escape and interact with intergalactic medium

High-energy neutrino production

Relativistic protons!!



Our galaxy
Star-forming Galaxy
AGN winds
Low-energy radiogalaxies (FRO)



Protons accelerated inside the AGN wind escape and interact with intergalactic medium

High-energy neutrino production

Relativistic protons!!



Our galaxy
Star-forming Galaxy
AGN winds
Low-energy radiogalaxies (FRO)



Protons accelerated inside the **jet** escape and interact with intergalactic medium

High-energy neutrino production

Relativistic protons!!



Our galaxy
Star-forming Galaxy
AGN winds
Low-energy radiogalaxies (FRO)

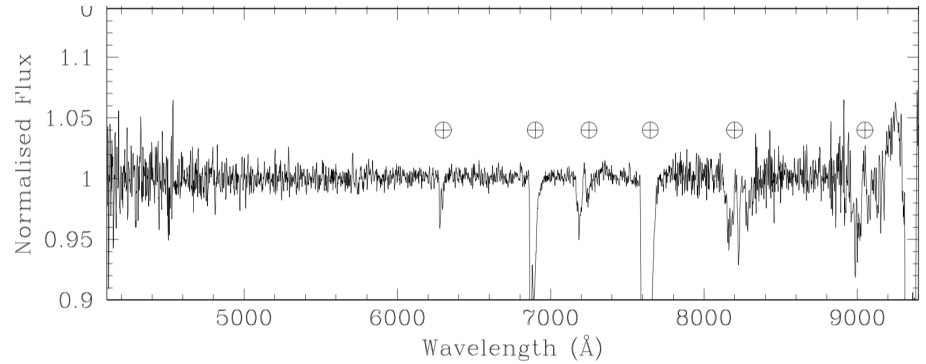
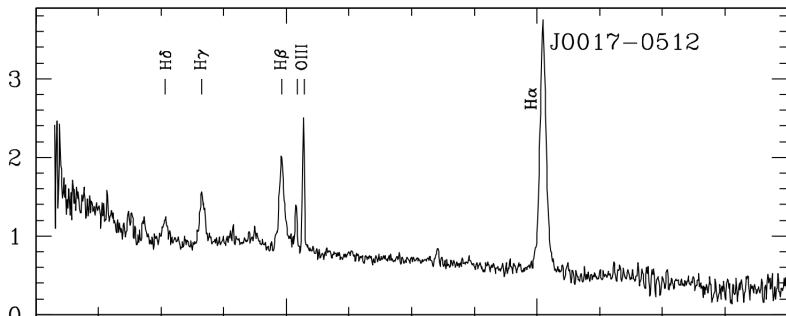


Jets
GRBs
Blazars

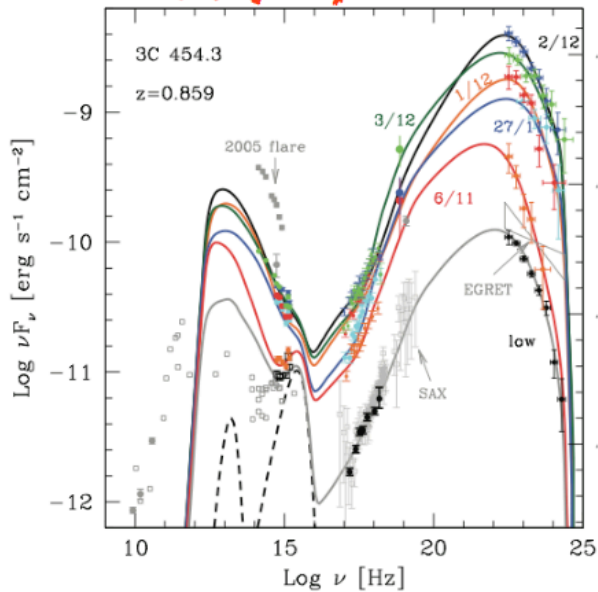
Blazars

FSRQ

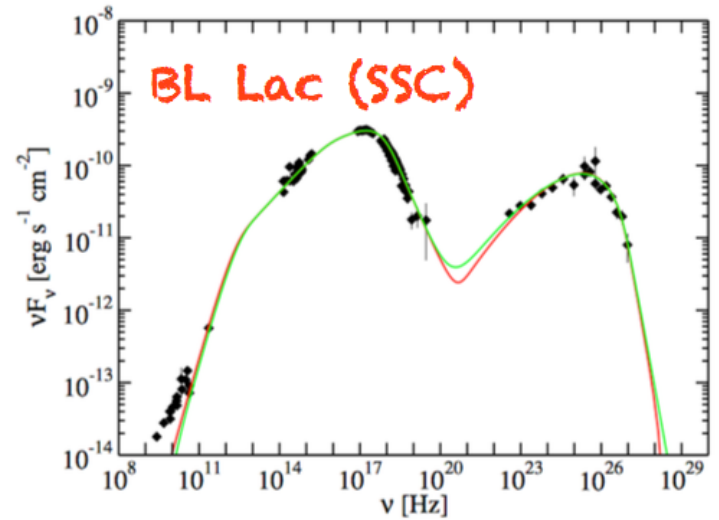
BL Lac



FSRQ (EC) Bonnoli et al. 2011

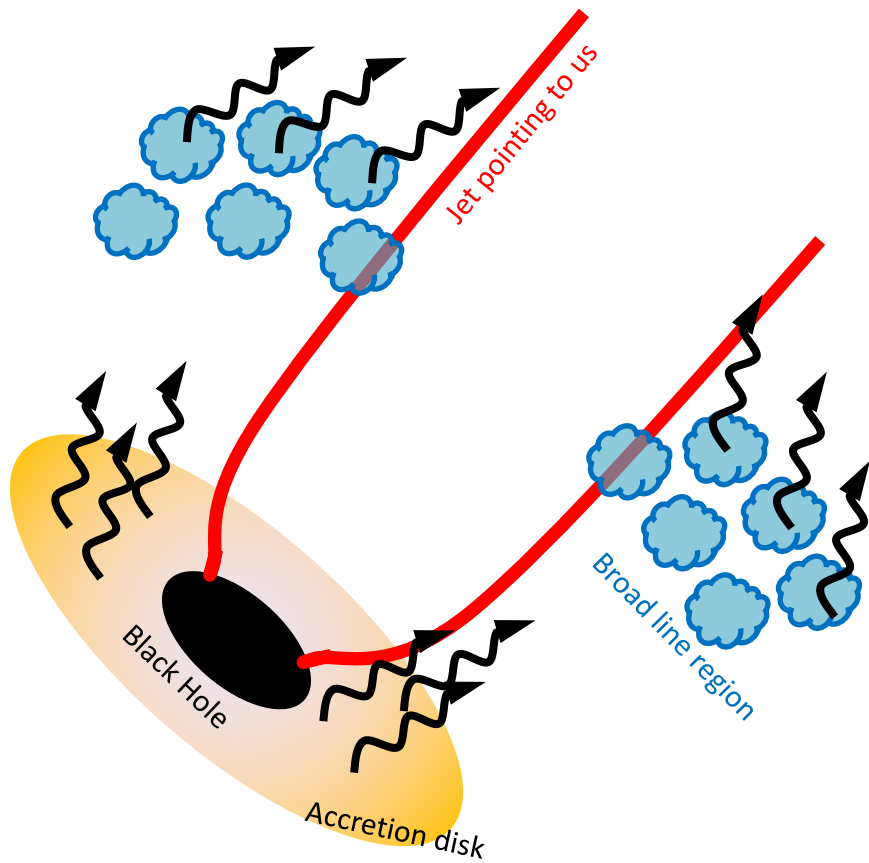


Abdo et al. 2011

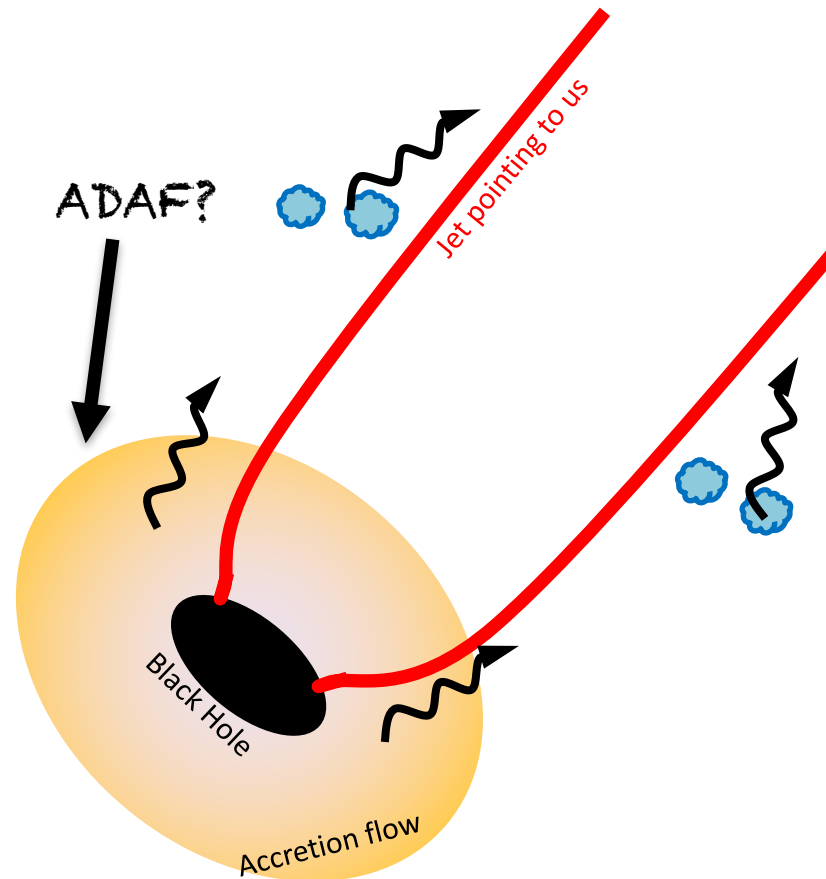


Blazars

FSRQ



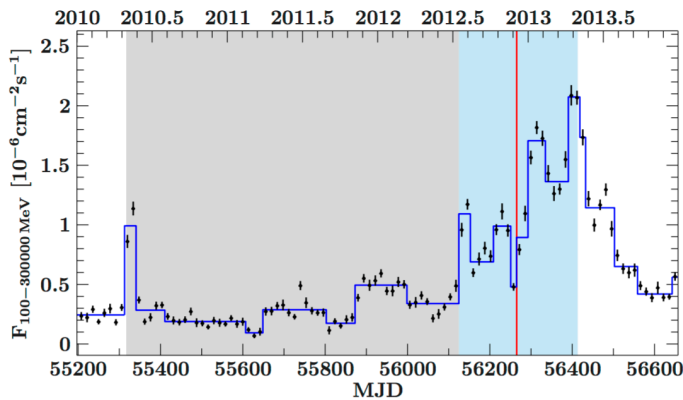
BL Lac



Are Blazars detectable by IceCube?

FSRQ

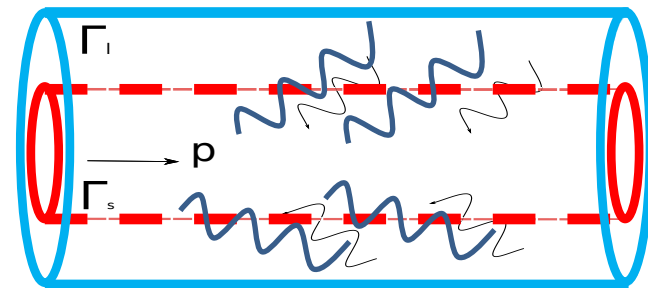
- ✓ Possible correlation between one neutrino event and a γ -ray flare of a FSRQ object (Kadler et al. 2016).



- ✗ EM- ν emission can't be exclusively hadronic (Gao et al. 2017)
- ✗ Murase and Waxman 2016
- ✗ $p+\gamma$ reaction with UV photons of BLR produce neutrino spectra harder than that "IceCube spectrum"

BL Lac

- ✓ Padovani et al. 2016 (spatial correlation with γ -ray BL Lacs detected above 50GeV)
- ✓ Tavecchio et al. 2014 efficient neutrino production (spine-layer model only for high-energy emitting BL Lacs)



Ghisellini et al. 2005

Fermi 2FHL catalogue (sources emitting above 50GeV) is a good representation of these sources

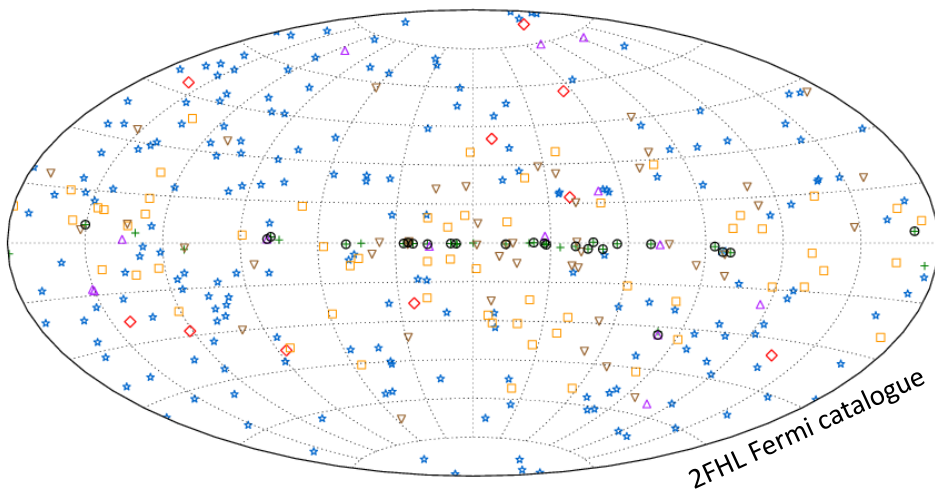
Righi et al. 2017 a

The model

Assumption 1:

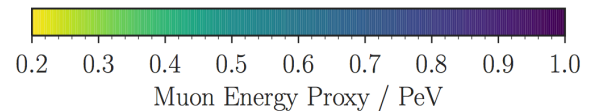
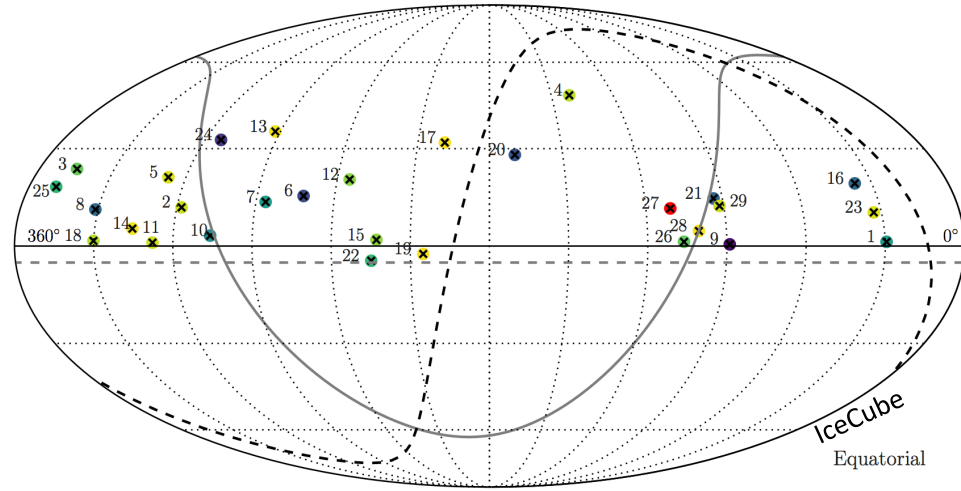
Only BL Lac objects of 2FHL catalogue contribute to ν_μ IC events.

Gamma-ray sky (50 GeV-2 TeV)



- | | | | |
|---|---|---|---|
| + | * | □ | ▽ |
| × | ◇ | △ | ○ |

High-energy neutrinos sky (>200 TeV)



Aartsen et al. 2016

Ackermann et al. 2015

Righi et al. 2017 a

The model

Assumption 1:

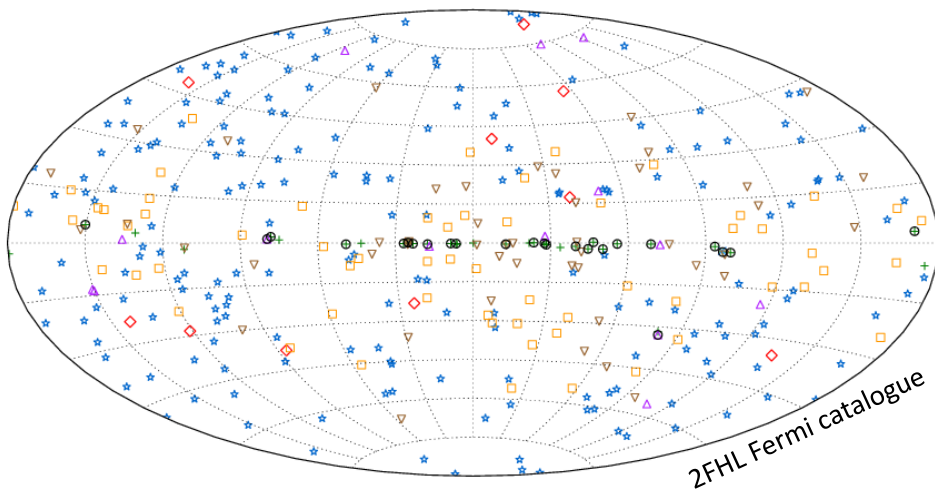
Only BL Lac objects of 2FHL catalogue contribute to ν_μ IC events.

Assumption 2:

Linear relation between γ -ray emission and neutrino emission.

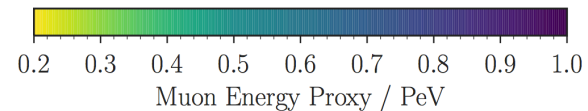
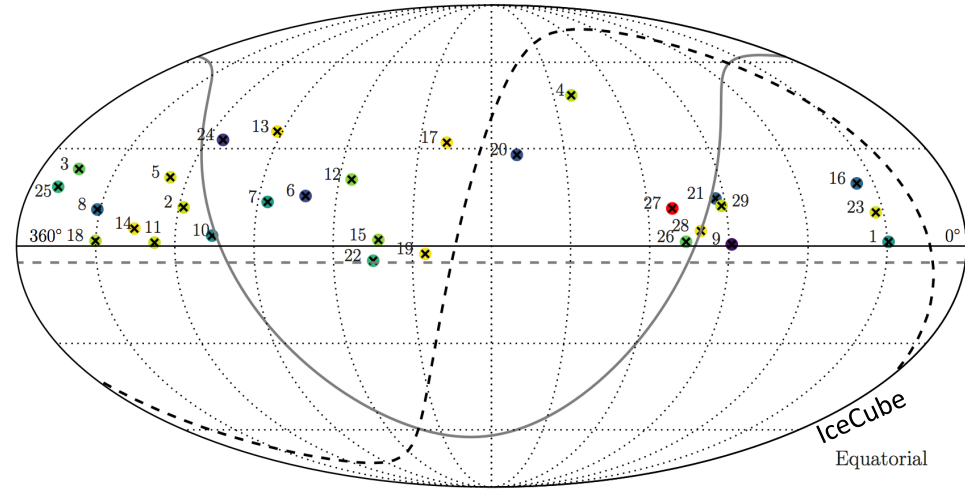
$$F_{\gamma i} = k F_{\nu i}$$

Gamma-ray sky (50 GeV-2 TeV)



| | | | | | | | |
|---|---------------|---|---------|---|--------------|---|--------------|
| + | SNRs and PWNe | * | BL Lacs | □ | Unc. Blazars | ▽ | Unassociated |
| × | Pulsars | ◇ | FSRQs | △ | Others | ○ | Extended |

High-energy neutrinos sky (>200 TeV)



Aartsen et al. 2016

Ackermann et al. 2015

Righi et al. 2017 a

The model

Assumption 1:

Only BL Lac objects of 2FHL catalogue contribute to ν_μ IC events.

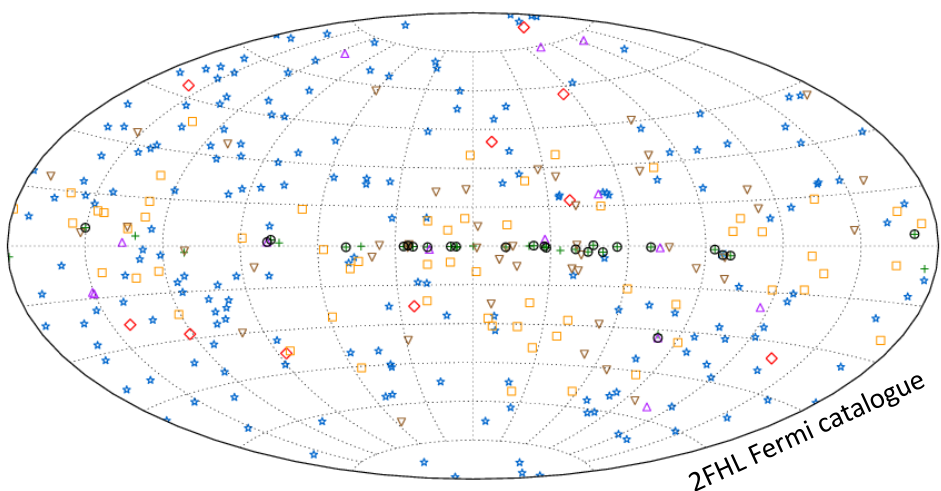
Assumption 2:

Linear relation between γ -ray emission and neutrino emission.

$$F_{\gamma i} = k F_{\nu i}$$

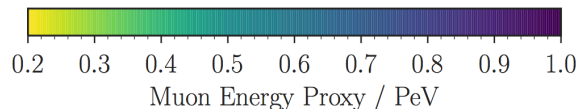
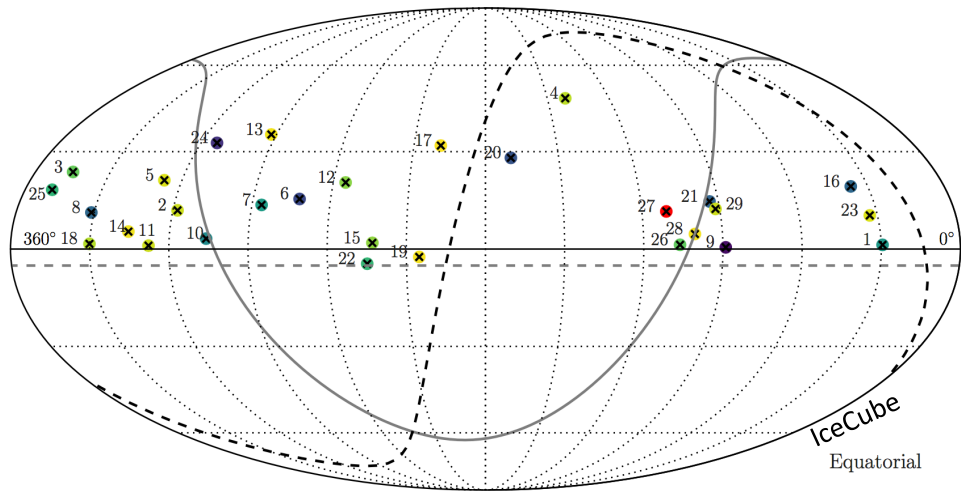
It's the same for all BL Lacs

Gamma-ray sky (50 GeV-2 TeV)



| | | | |
|---|---|---|---|
| + | * | □ | ▽ |
| x | ◇ | △ | ○ |

High-energy neutrinos sky (>200 TeV)



Ackermann et al. 2015

Aartsen et al. 2016

Righi et al. 2017 a

Results

$$N_\nu = \dot{N}_\nu T_{\text{exp}} = T_{\text{exp}} \int_{E_1}^{E_2} A_{\text{eff}}(E_\nu) \Phi_i(E_\nu) dE_\nu$$

IceCube

| 60° < δ < 90° | | FLUX | #ν |
|---------------|---------------------|------|------|
| 1 | 1ES1959+650 | 1.38 | 0.27 |
| 2 | 1ES0502+675 | 1.14 | 0.22 |
| 3 | S50716+71 | 0.44 | 0.08 |
| 4 | 1RXSJ013106.4+61203 | 0.25 | 0.05 |
| 5 | 4C+67.04 | 0.25 | 0.05 |
| 6 | Mkn180 | 0.24 | 0.05 |
| 7 | MS0737.9+7441 | 0.13 | 0.02 |
| 8 | RXJ0805.4+7534 | 0.08 | 0.02 |
| 9 | S40954+65 | 0.07 | 0.01 |
| 10 | S41749+70 | 0.07 | 0.01 |
| 30° < δ < 60° | | | |
| 11 | Mkn421 | 8.77 | 4.89 |
| 12 | Mkn501 | 3.41 | 1.90 |
| 13 | PG1218+304 | 0.92 | 0.52 |
| 14 | 3C66A | 0.87 | 0.49 |
| 15 | 1H1013+498 | 0.87 | 0.49 |
| 16 | 1ES0033+595 | 0.82 | 0.46 |
| 17 | 1ES2344+514 | 0.69 | 0.39 |
| 18 | 1ES1215+303 | 0.52 | 0.29 |
| 19 | B32247+381 | 0.37 | 0.21 |
| 20 | B30133+388 | 0.35 | 0.19 |
| 0° < δ < 30° | | | |
| 21 | PG1553+113 | 1.89 | 2.47 |
| 22 | PKS1424+240 | 1.00 | 1.30 |
| 23 | PG1218+304 | 0.92 | 1.20 |
| 24 | TXS0518+211 | 0.87 | 1.14 |
| 25 | 1ES0647+250 | 0.75 | 0.99 |
| 26 | 1ES1215+303 | 0.52 | 0.69 |
| 27 | RXJ0648.7+1516 | 0.45 | 0.59 |
| 28 | 1RXSJ194246.3+10333 | 0.41 | 0.54 |
| 29 | RBS0413 | 0.32 | 0.42 |
| 30 | 1H1720+117 | 0.25 | 0.33 |

Km3Net (prediction)

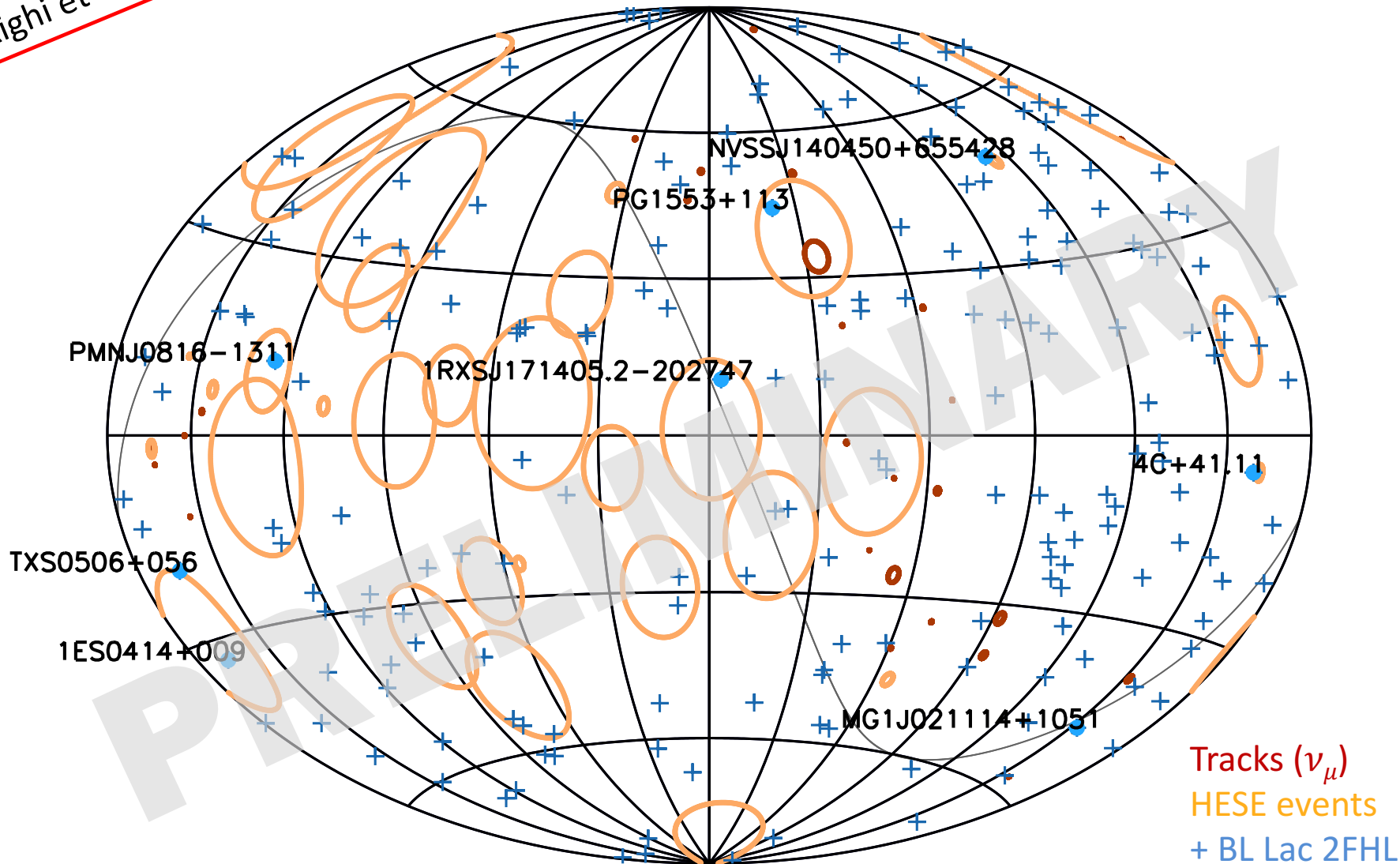
| | Name | F_ν | R_ν | Visibility at horizon | R_ν | Visibility at 10° |
|-----------------|---------------------|---------|---------|-----------------------|---------|-------------------|
| 1 | Mkn421 | 8.77 | 4.59 | 0.30 | 5.80 | 0.39 |
| 2 | PKS2155-304 | 2.15 | 2.23 | 0.60 | 2.53 | 0.69 |
| 3 | Mkn501 | 3.41 | 1.65 | 0.28 | 2.26 | 0.39 |
| 4 | PG1553+113 | 1.89 | 1.42 | 0.44 | 1.66 | 0.51 |
| 5 | PKS0447-439 | 0.76 | 0.87 | 0.67 | 1.02 | 0.79 |
| 6 | PKS1424+240 | 1.00 | 0.67 | 0.39 | 0.79 | 0.46 |
| 7 | PKS2005-489 | 0.51 | 0.63 | 0.72 | 0.75 | 0.86 |
| 8 | TXS0518+211 | 0.87 | 0.59 | 0.39 | 0.72 | 0.48 |
| 9 | PG1218+304 | 0.92 | 0.55 | 0.44 | 0.69 | 0.44 |
| 10 | 1ES0647+250 | 0.75 | 0.47 | 0.36 | 0.60 | 0.46 |
| 11 | 3C66A | 0.87 | 0.38 | 0.25 | 0.54 | 0.36 |
| 12 | 1RXSJ054357.3-55320 | 0.30 | 0.40 | 0.78 | 0.52 | 1.00 |
| 13 | PKS0301-243 | 0.43 | 0.44 | 0.59 | 0.49 | 0.66 |
| 14 | 1H1914-194 | 0.45 | 0.44 | 0.57 | 0.49 | 0.63 |
| 15 ^a | 1H1013+498 | 0.87 | - | - | 0.48 | 0.32 |
| 15 ^b | 1RXSJ194246.3+10333 | 0.41 | 0.32 | 0.45 | - | - |
| 16 | PKS1440-389 | 0.36 | 0.41 | 0.66 | 0.47 | 0.76 |
| 17 | 1ES0347-121 | 0.39 | 0.35 | 0.53 | 0.40 | 0.60 |
| 18 | 1ES1215+303 | 0.52 | 0.31 | 0.34 | 0.39 | 0.44 |
| 19 | 1RXSJ101015.9-31190 | 0.32 | 0.34 | 0.60 | 0.39 | 0.69 |
| 20 | RXJ0648.7+1516 | 0.45 | 0.33 | 0.42 | 0.38 | 0.49 |

Collaboration for simulation ongoing

10⁻⁸ GeV/cm²s yr⁻¹

Righi et al. submitted

Lacs candidates

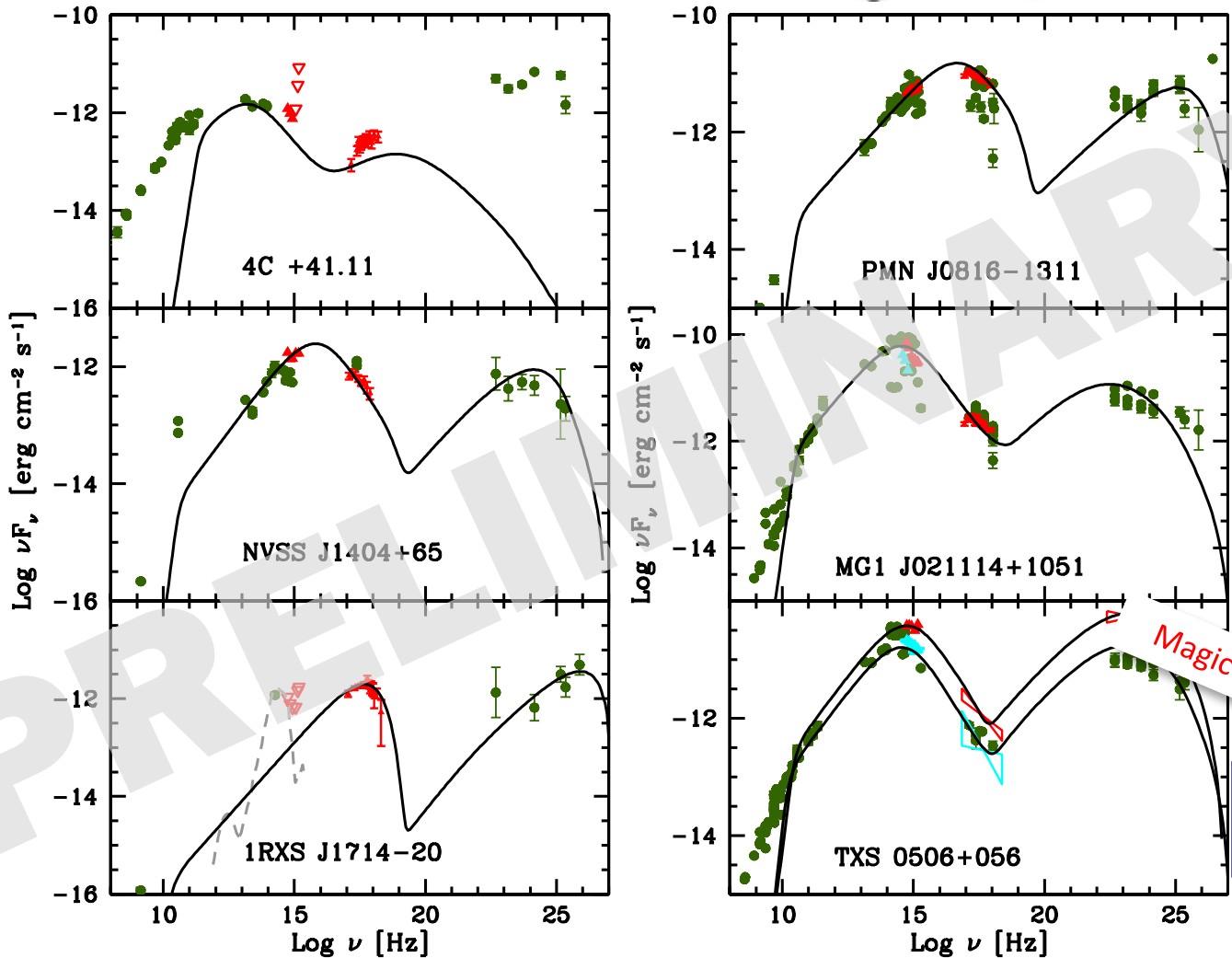


8 BL Lac object with a spatial correlation with a track or an HESE event.

Righi et al. submitted

Lacs candidates

Data analysis: **REM** *Swift*





Work in progress

Why IceCube haven't detect the brightest **Mkn421** or **Mkn501** yet?

They are proto-typical **HSP** with indications for the existence of Spine-Layer structure...

...**TXS0506+056** is **ISP** (for which SL structure is not yet convincingly proven)...

COMING SOON

Take home messages

- Blazar are good candidates to produce high-energy neutrinos!
- **TXS 0506+056** is very intriguing...
Stay tuned!
- The "problem of **MKN421**" is a question which have yet to be resolved.

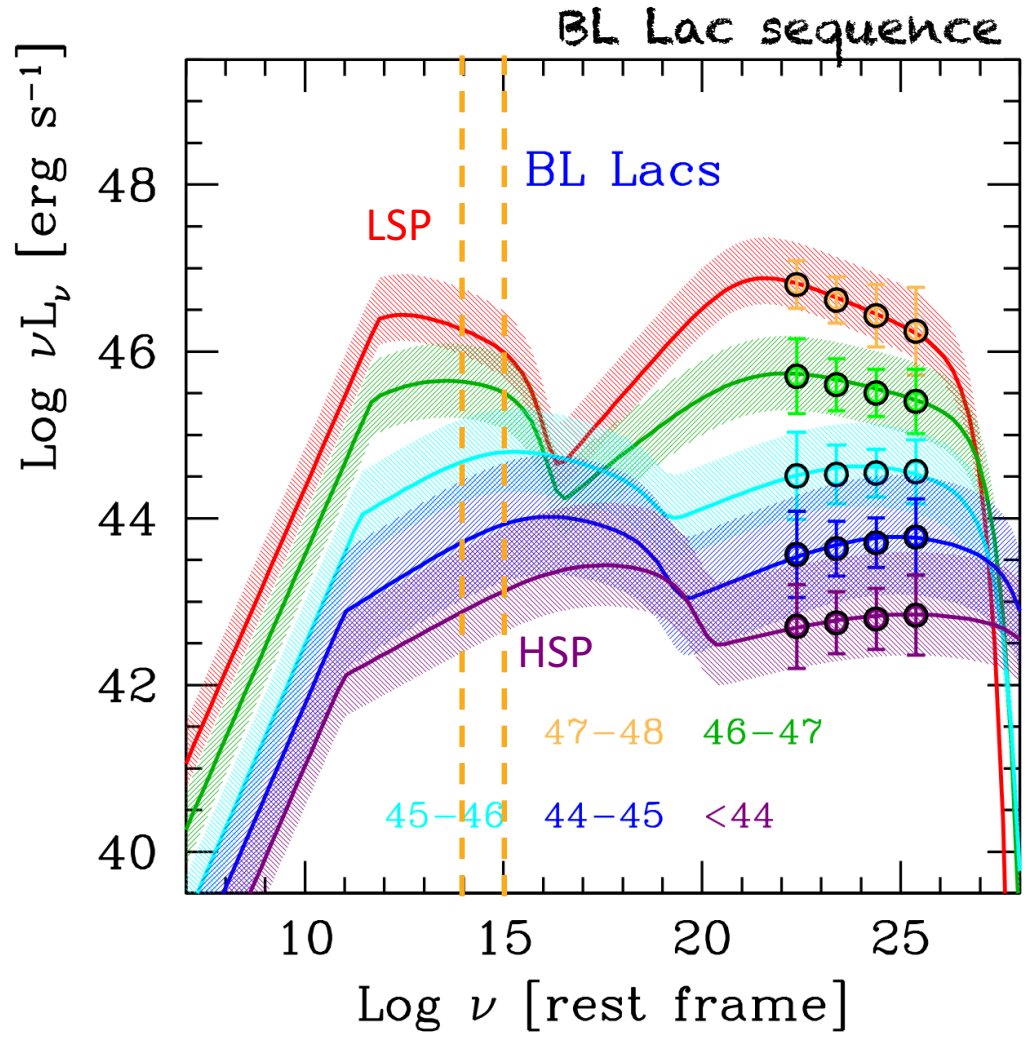
THANKS!



Work in progress

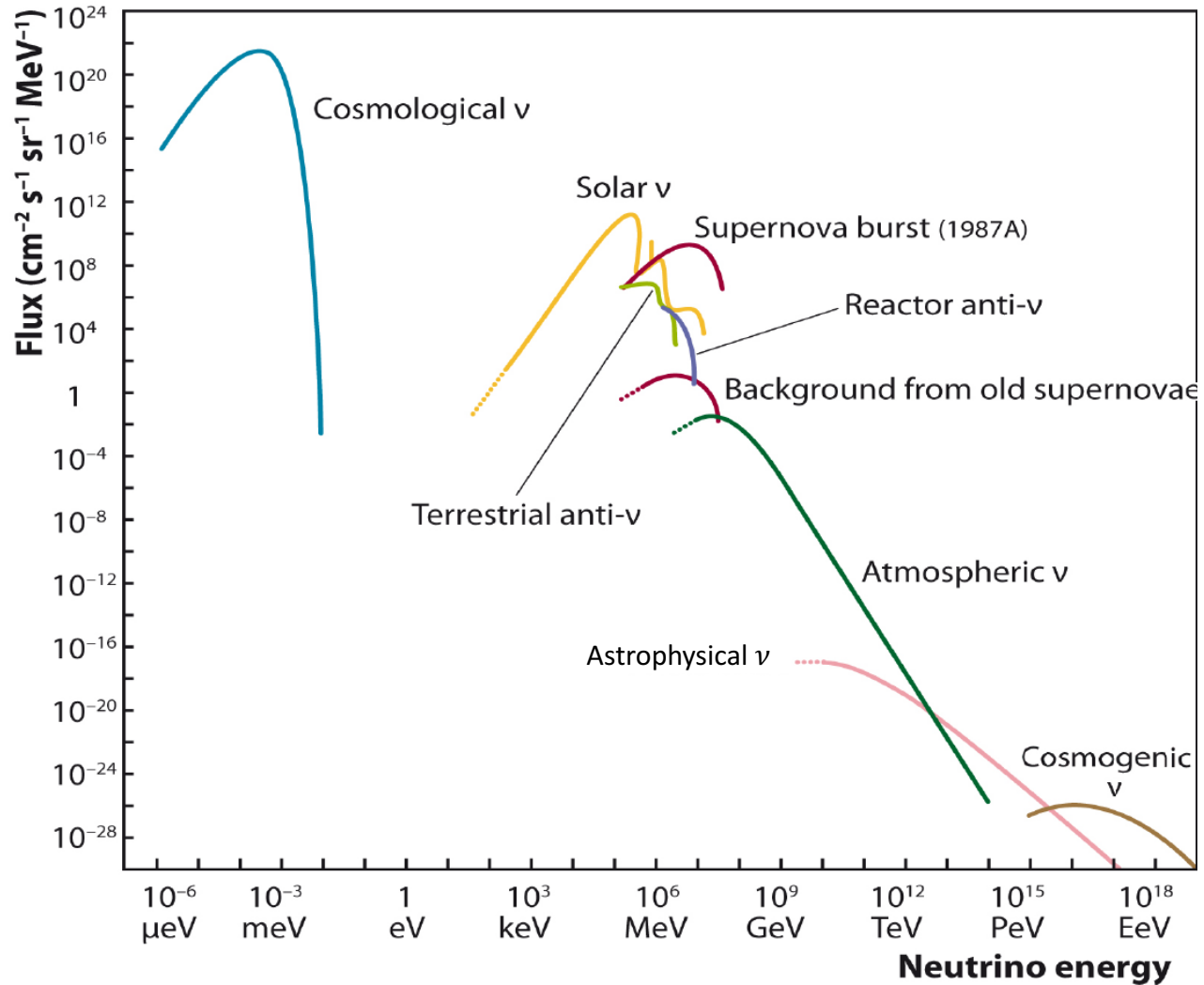
LSP: $\nu_{peak}^S < 10^{14} \text{ Hz}$
 ISP: $10^{14} \text{ Hz} < \nu_{peak}^S < 10^{15} \text{ Hz}$
 HSP: $\nu_{peak}^S > 10^{15} \text{ Hz}$

Ackermann et al. 2015 - 3LAC

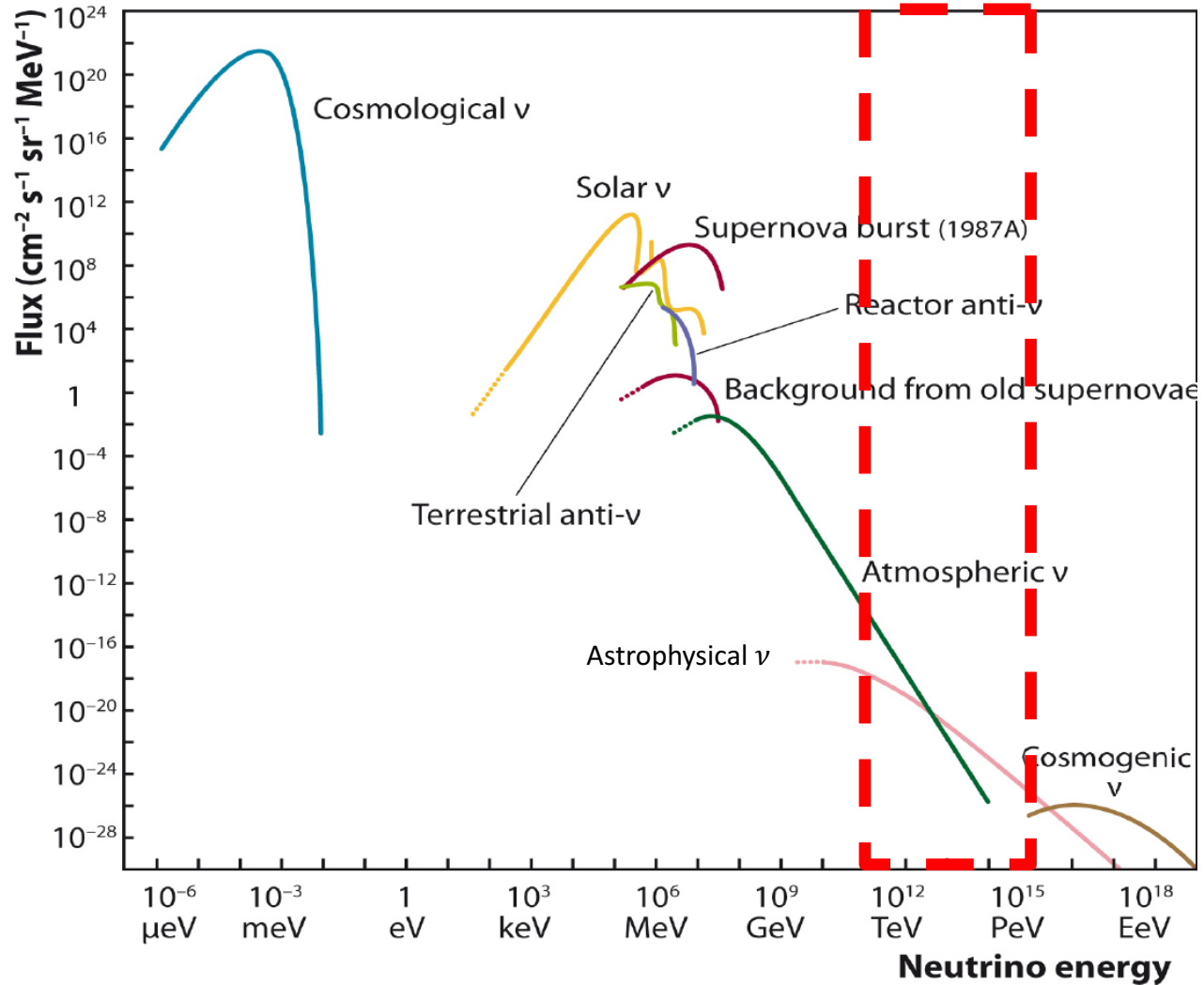


Thanks to G. Ghisellini

Neutrino flux

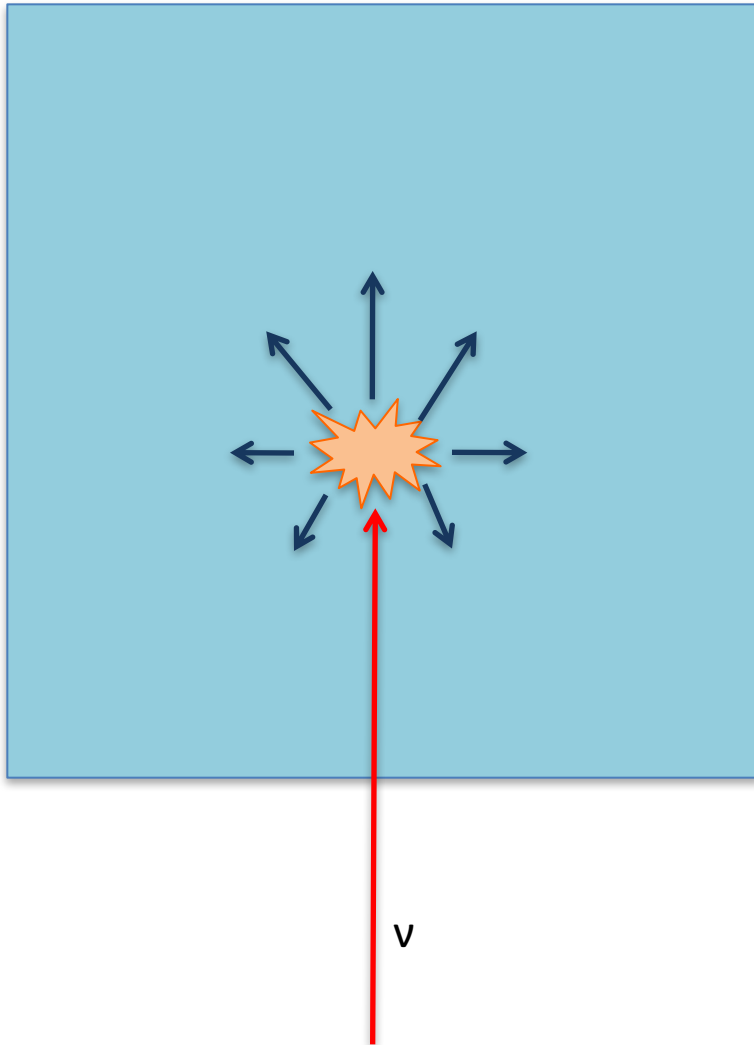


Neutrino flux

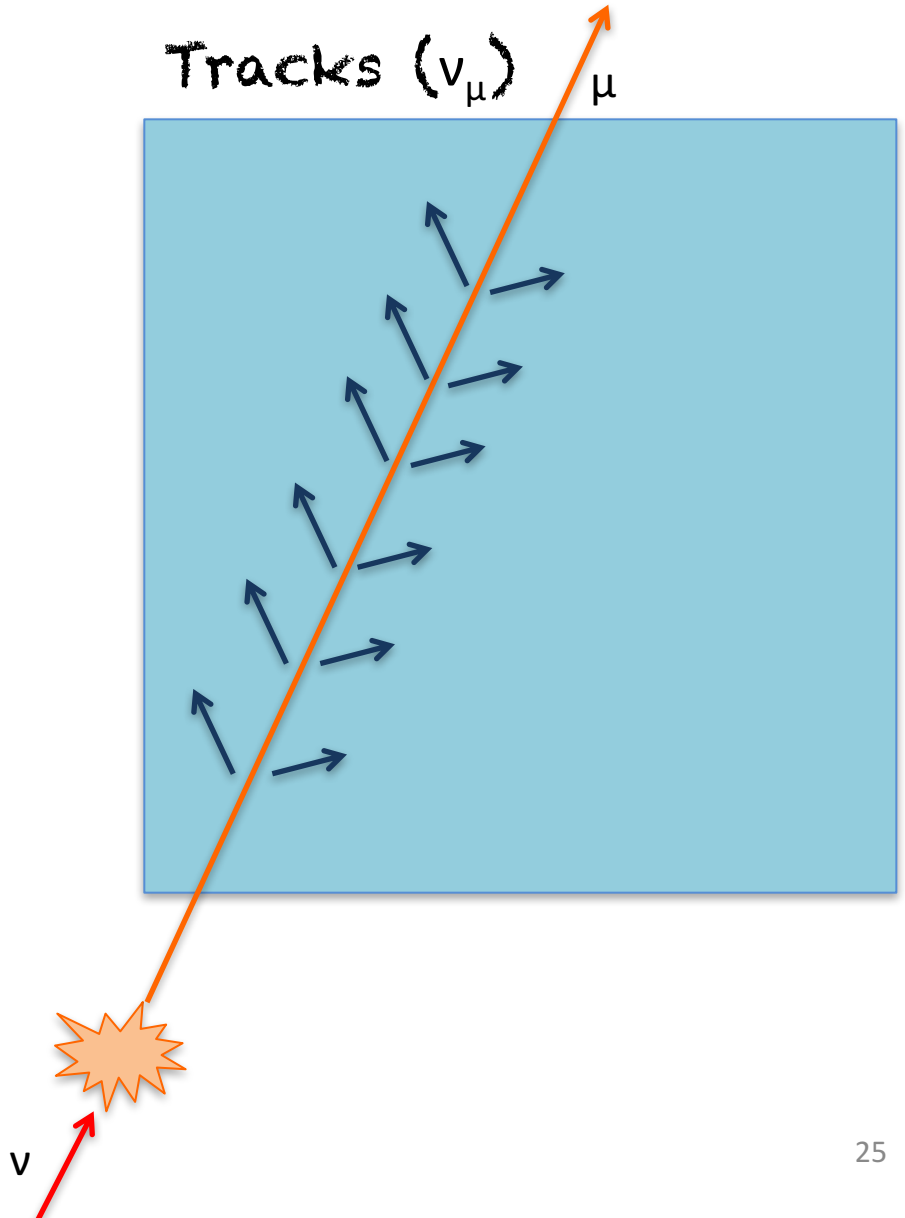


Different signature

Cascade (ν_e, ν_μ, ν_τ)



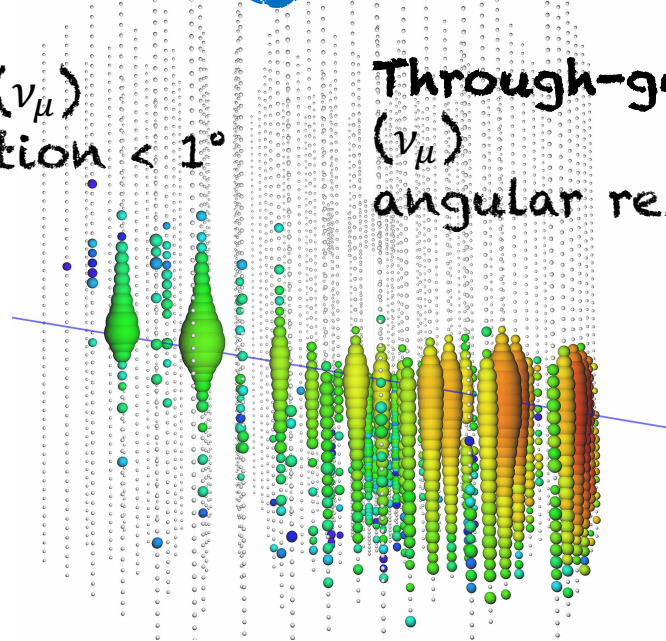
Tracks (ν_μ) μ



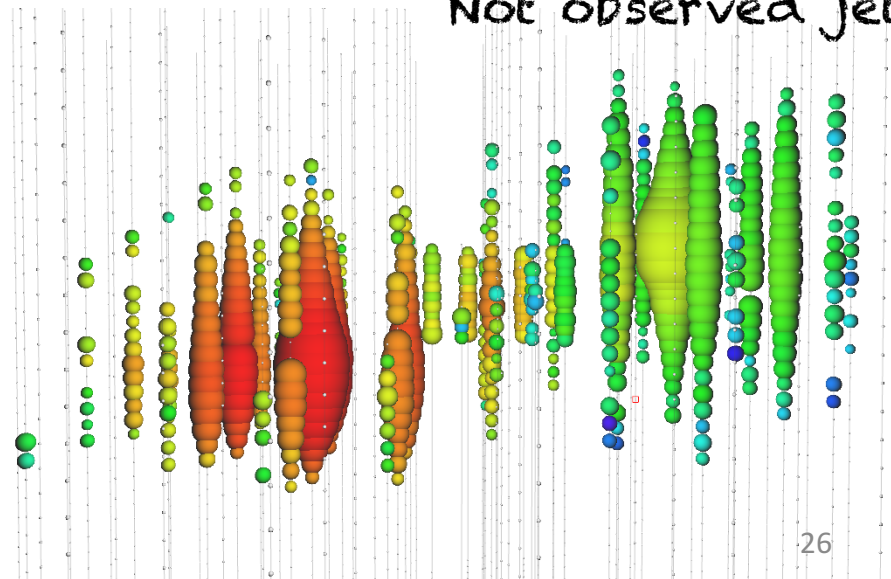
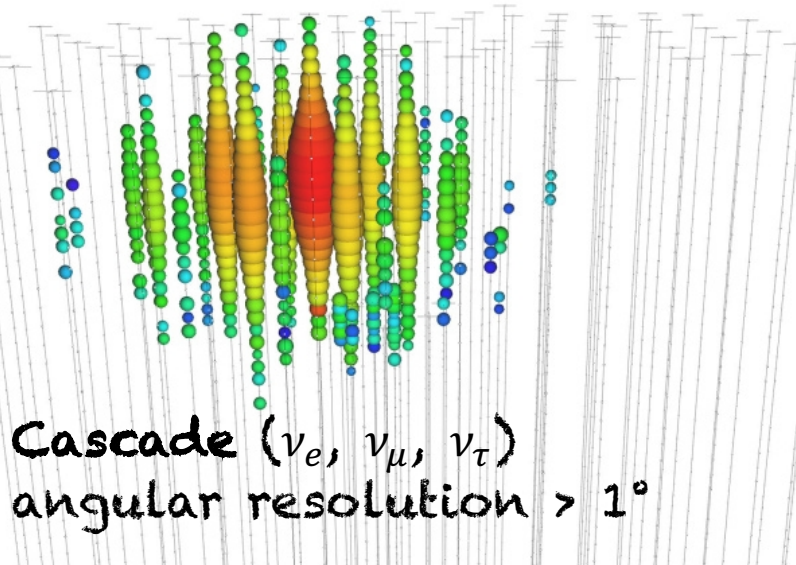
Neutrino signature in ice

Starting track (ν_μ)
angular resolution $< 1^\circ$

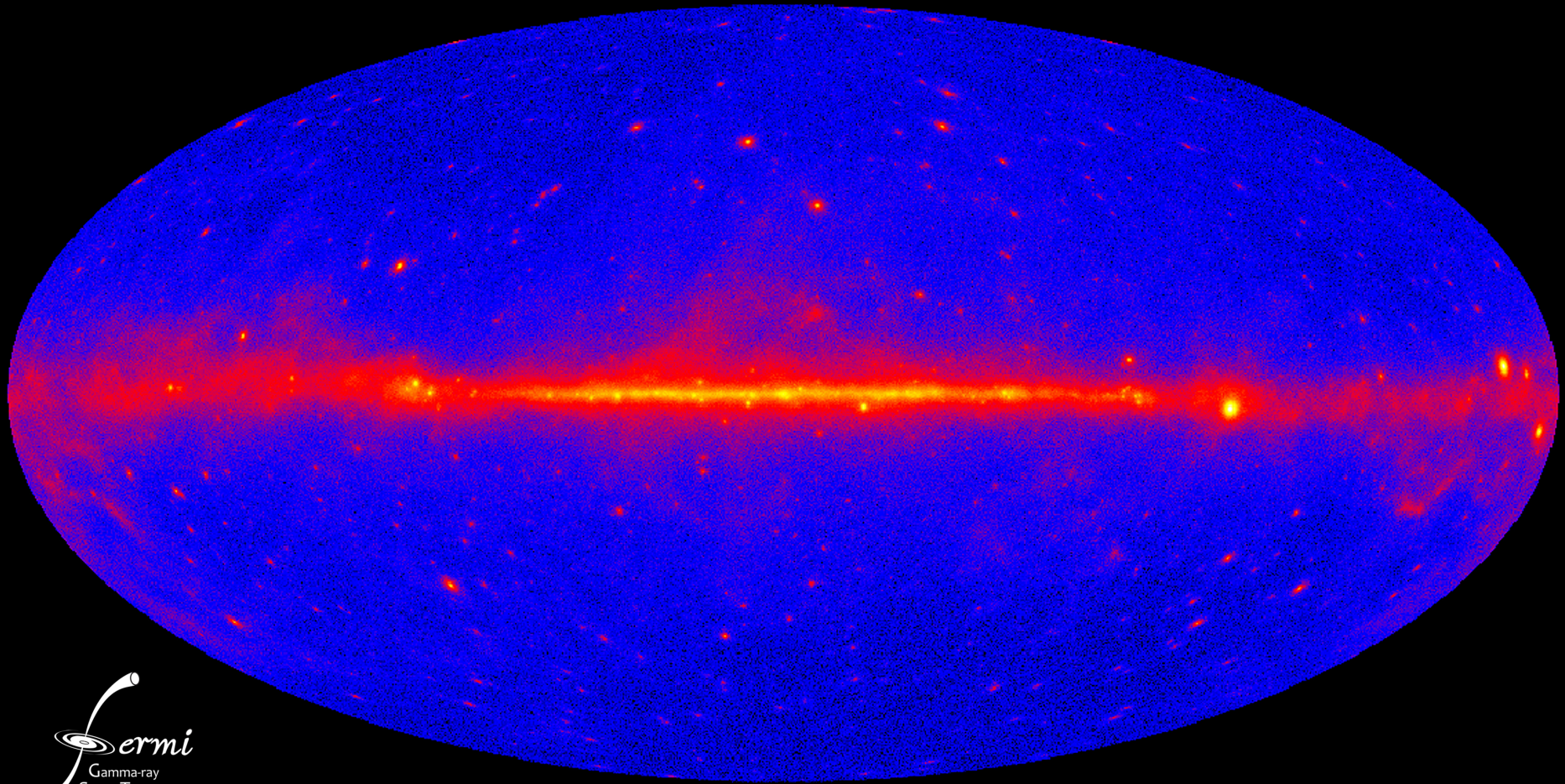
Through-going track (ν_μ)
angular resolution $< 1^\circ$



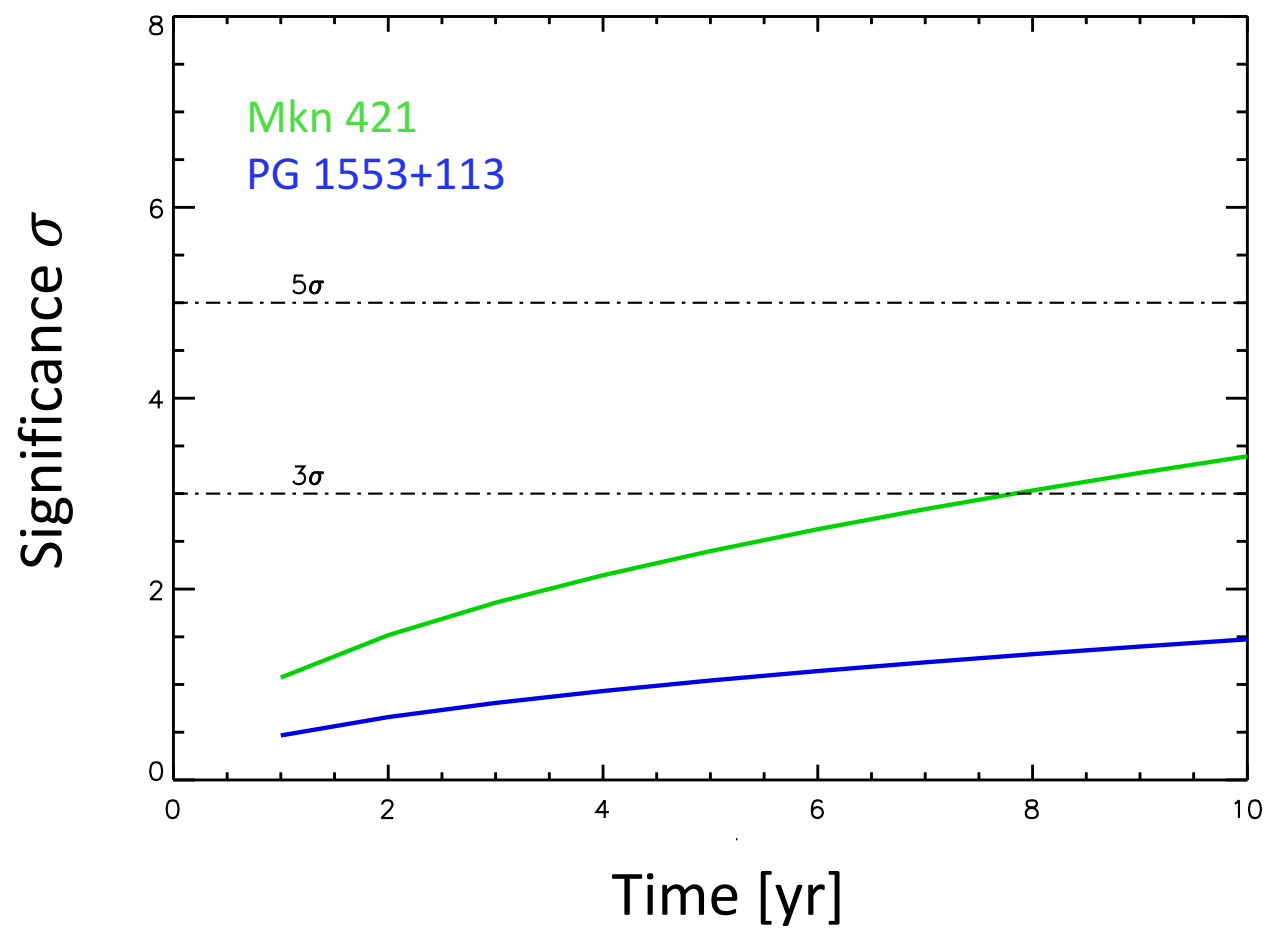
Double bang (ν_τ)
Not observed jet



>60% extragal due to Blazar!



Detectability



Assuming 30% efficiency of the detector
This analysis includes the background!

Detectability

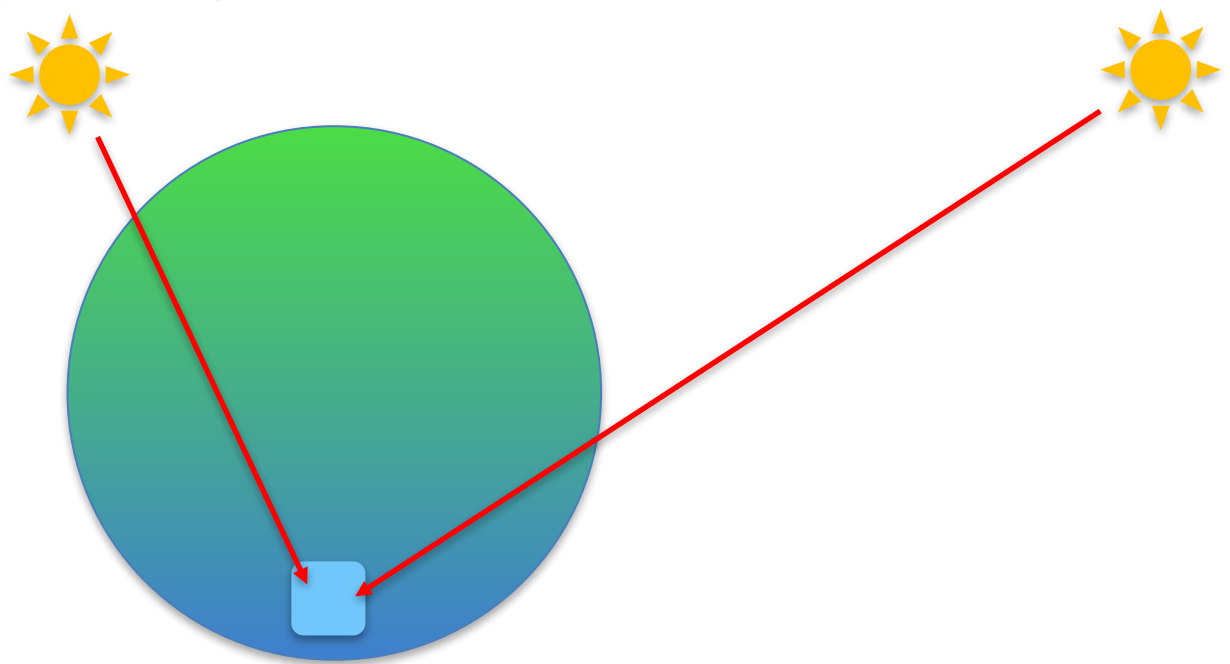
average muon energy-loss rate

Neutrino flux for each source

Charge current cross section

Attenuation due to Earth

$$\frac{d\dot{N}}{dE_\mu} = \frac{1}{\alpha + \beta E_\mu} \frac{A}{m_p} \int_{E_\mu}^{E_{\nu max}} \phi(E_\nu) \sigma_{CC}(E_\nu) e^{-\tau(x, E_\nu)} dE_\nu$$

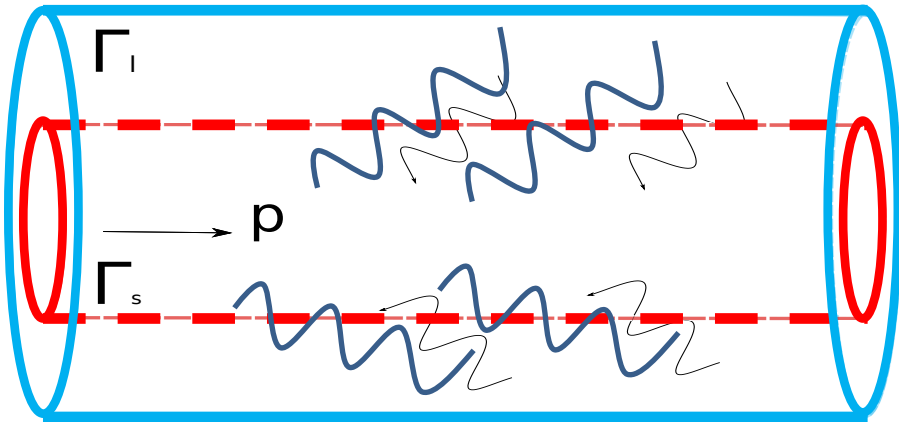


Spine-Layer Model

$$\Gamma_s = 15 - 20$$

$$\Gamma_l = 3 - 5$$

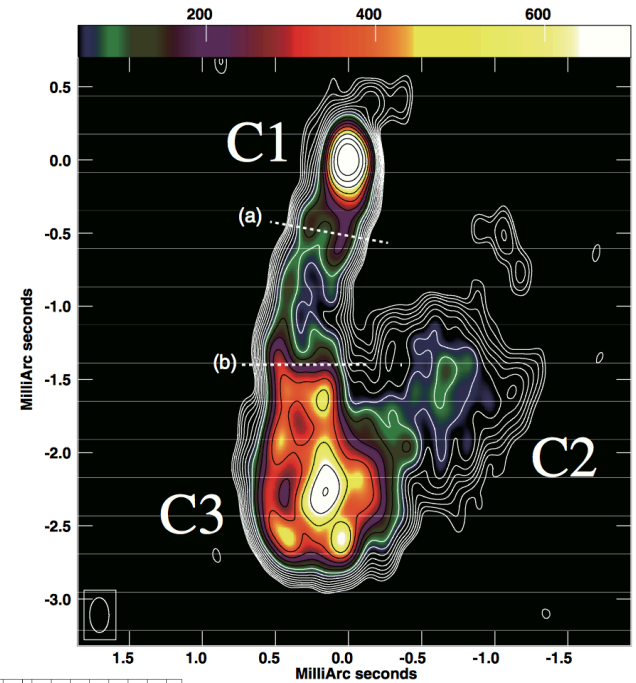
The relative motion of the two components leads to the amplification of the radiation field of the layer as observed in the spine reference frame.



Ghisellini et al. 2005

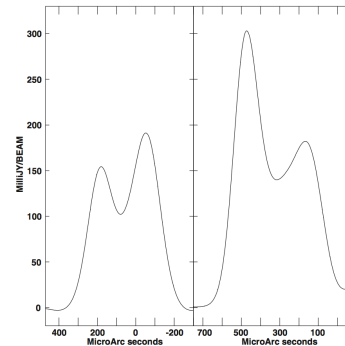
Tavecchio & Ghisellini 2008, 2014

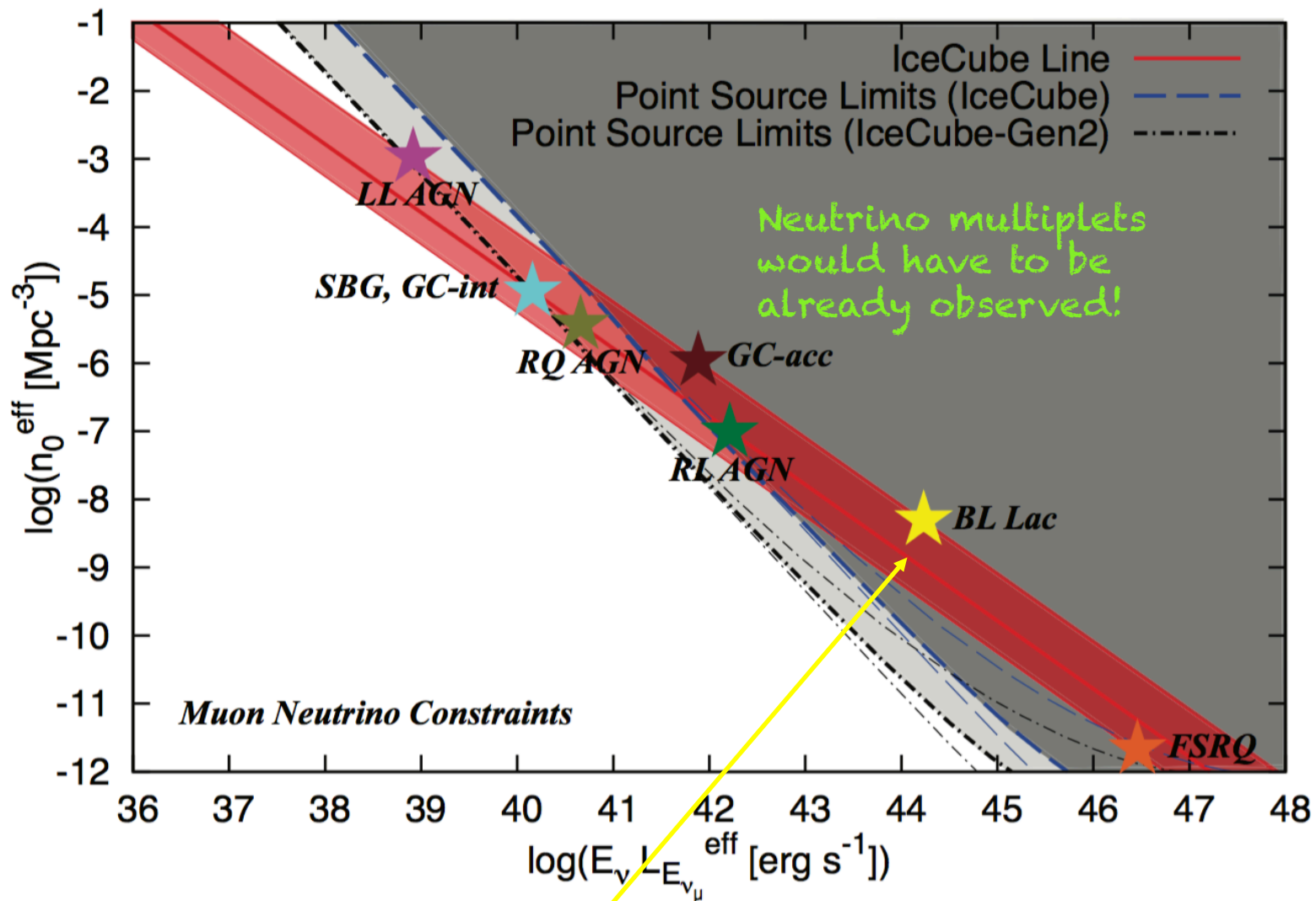
the weakly beamed emission of the layer could dominate the emission from misaligned radiogalaxies



Nagai et al. 2014

Giovannini et al. 2015





BL Lac of 1FGL (not representative of HBL)

Theoretical framework

- Leptonic scenario for the SED
 - EM and ν outputs derive from two different (**but not independent!**) channels
 - Neutrino luminosity: $L_\nu = \epsilon_p Q'_p \delta_S^4$
 - IC luminosity: $L_\gamma = \epsilon_e Q'_e \delta_S^4$
- $Q'_{p,e}$ CR, electrons injected power
- $\frac{F_\nu}{F_\gamma} = \frac{L_\nu}{L_\gamma} = \frac{\epsilon_p Q'_p}{\epsilon_e Q'_e}$
 - ϵ_p and ϵ_e depend on the same photon field
 - Q'_p and Q'_e depend on the total power P_{jet}
 - $\frac{F_\nu}{F_\gamma} \approx const.$ the same in all HBL.

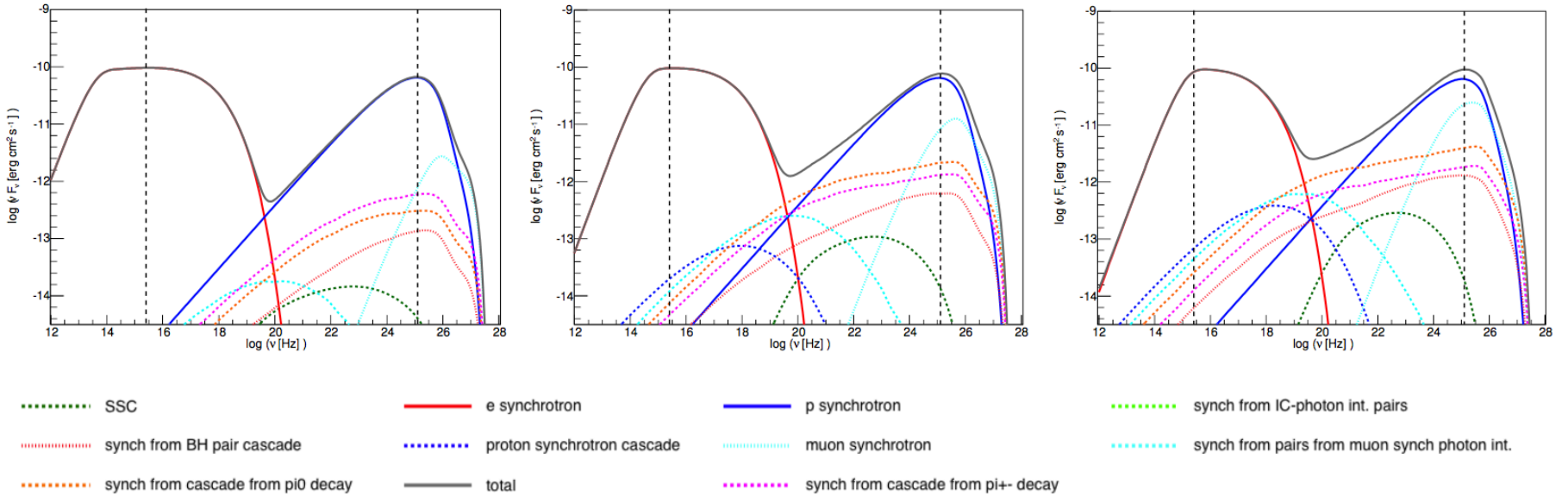
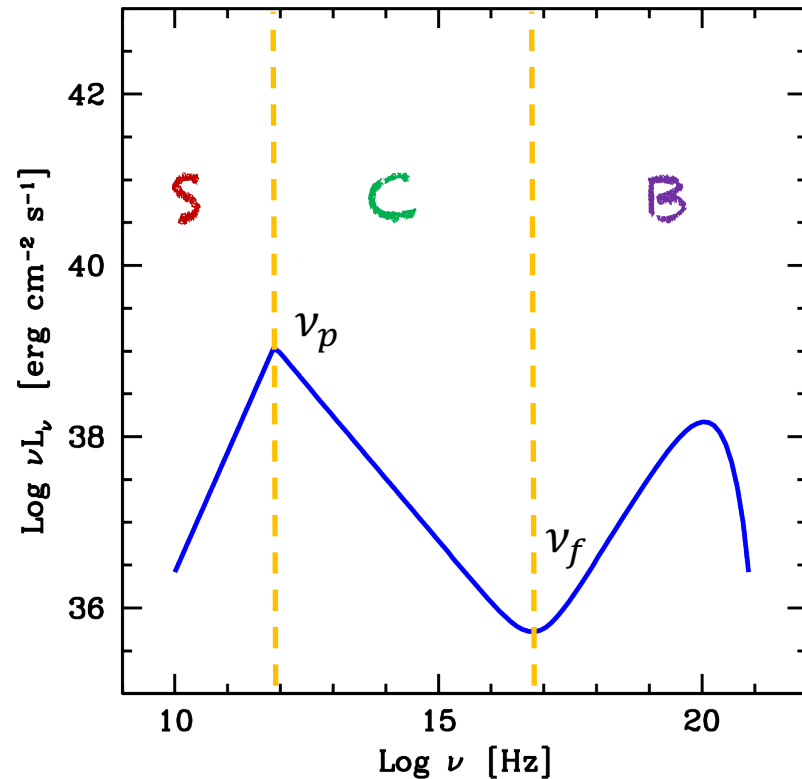


Fig. 2. Variation in the modelled SED when moving along the diagonal in $\log R$ - $\log B$ space. From left to right, models with $\log B[G] = 0.5, 1.5, 2.0$ are shown. Particle densities are adjusted to maintain the same overall flux level between the different models. Solid red and blue lines indicate the electron and proton synchrotron emission. The dotted and dashed lines show muon-synchrotron emission at the highest energies, and the SSC and muon-synchrotron cascade components at lower energies, as indicated in the legend. The VHE spectrum is absorbed by the EBL, assuming a redshift of 0.116, corresponding to the source PKS 2155-304. The spectral index n_1 is chosen to be 1.9. The two dashed vertical lines are there to guide the eye by marking the approximate peak positions of the model in the central figure.

Advection Dominated Accretion Flow (ADAF)

2-temperature structure, with hot ions holding most of the energy and transferring it inefficiently to the electrons that produce most of the radiation.



S: $\nu < \nu_p$ ciclo-synchrotron emission

C: $\nu_p < \nu < \nu_f$ comptonisation of **S**

B: $\nu > \nu_f$ bremsstrahlung emission

After ν_p the synchrotron spectrum falls exponentially

Average energy of a photon for saturated comptonization in the Wien regime $h\nu_f = 3kT_e$

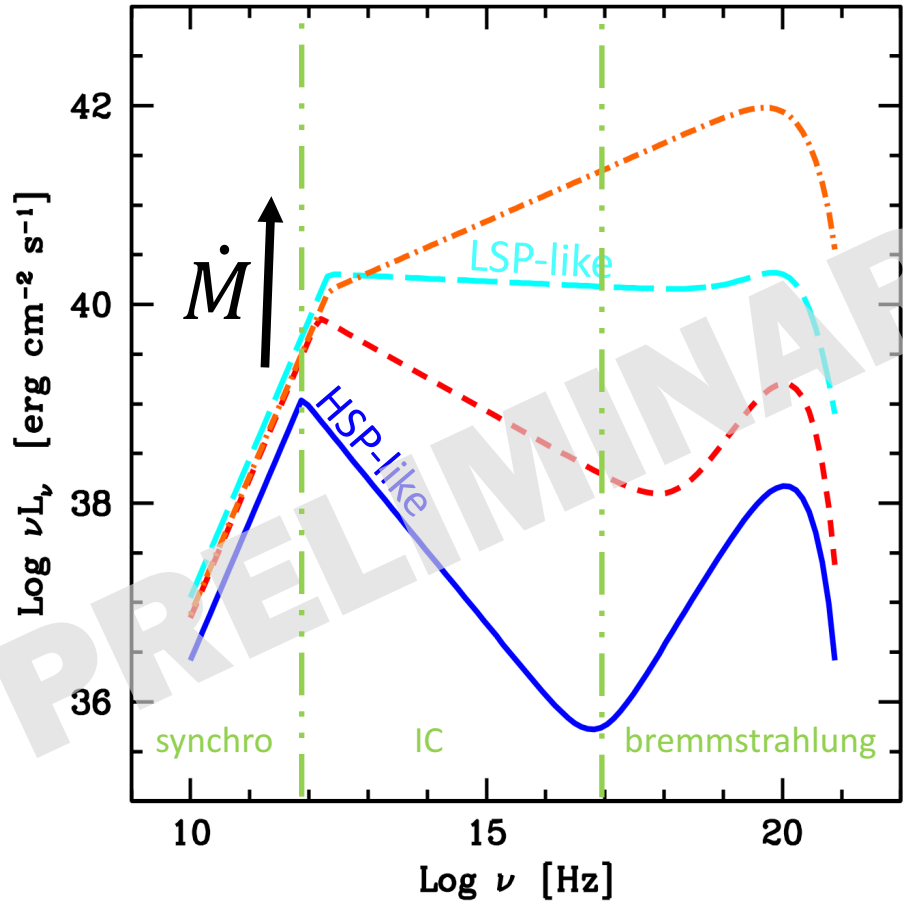
MAHADEVAN 97
Narayanan & Yi 95a, 95b



Work in progress

ADAF model
Narayan & Yi 95a, 95b
MAHADEVAN 97

$$L_{jet} \propto L_{disk}$$
$$L_{disk} \propto \dot{M}^2$$



The ADAF spectrum depends on \dot{M} .

LSP: red peak \rightarrow high accretion rate

HSP: blue peak \rightarrow low accretion rate



Work in progress

ADAF model

Pound for CR luminosity,
the neutrino luminosity
decrease drastically in
case of HSP!

This lack can
explain the
potential detection
of TXS0506+056
and the non-
detection of
Mkn421.

